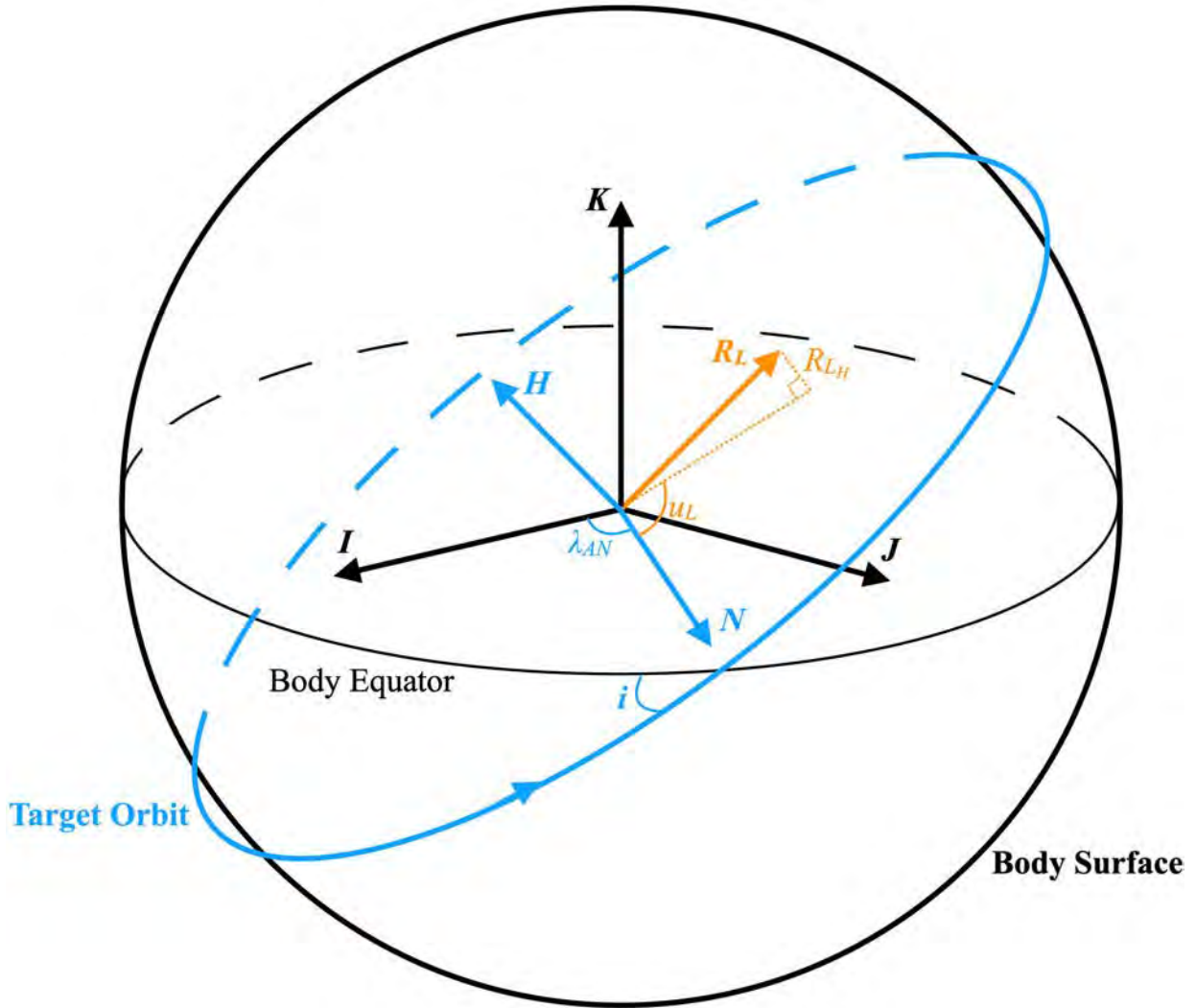


# Launch Site Geometric In-Plane Time On A Target Orbit

Consider a time-independent unit vector of launch site position  $\mathbf{R}_L$  in the equator-prime meridian (EPM) coordinate system centered on a specified gravitating launch body.<sup>1</sup> Although EPM principal axes rotate with this body at angular rate  $\omega$ , they are assumed fixed in inertial space at a specified epoch such as a candidate launch time  $t_L$ .

This paper seeks to iteratively compute  $t_L$  based on the geometry in Figure 1 such that  $\mathbf{R}_L$  lies in the orbit plane of a target vehicle whose ephemeris centered on the launch body is provided. Thus, at any  $t_L$ , the target's EPM position  $\mathbf{r}$  and EPM velocity  $\mathbf{v}$  with respect to the launch body are available.



**Figure 1. The launch body-centered launch site position unit vector  $\mathbf{R}_L$  is fixed with respect to the EPM coordinate system defined by principal axes  $\mathbf{I} \times \mathbf{J} = \mathbf{K}$ . In contrast, the target orbit plane is nearly fixed in inertial space such that  $\lambda_{AN}$  increases with time as EPM coordinates rotate about  $\mathbf{K}$  at the angular rate  $\omega$ . At epochs when the component of  $\mathbf{R}_L$  along  $\mathbf{H}$  ( $\mathbf{R}_{LH}$ ) is zero, a geometric target orbit in-plane time occurs.**

<sup>1</sup> Cartesian EPM principal axes have  $\mathbf{I}$  directed at zero latitude and longitude;  $\mathbf{J}$  directed at zero latitude, 90° E longitude; and  $\mathbf{K}$  directed at 90° N latitude (the north rotational pole) with  $\mathbf{I} \times \mathbf{J} = \mathbf{K}$  in the right-handed convention.

## Launch Site Geometric In-Plane Time On A Target Orbit

Common to all  $t_L$  iterations is the launch site's EPM longitude  $\lambda_L = \text{atan2}(\mathbf{R}_L \cdot \mathbf{J}, \mathbf{R}_L \cdot \mathbf{I}) \equiv \text{atan2}(R_{L_J}, R_{L_I})$ .<sup>2</sup>

A  $t_L$  iteration begins by fetching  $\mathbf{r}$  and  $\mathbf{v}$  from the target ephemeris at the current launch time estimate  $t_0$ . The EPM unit vector  $\mathbf{H}$  normal to the target orbit plane is first computed.

$$\mathbf{H} = \text{unit}(\mathbf{r} \times \mathbf{v}) \quad (1)$$

Launch site geometric latitude on the target orbit plane is given by Equation 2. Evaluating Equation 2 is optional, as  $\varphi_L$  is not explicitly used elsewhere in the iteration. Its chief use would likely be for informative display purposes.

$$\varphi_L = \text{asin}(R_{L_H}) = \text{asin}(\mathbf{R}_L \cdot \mathbf{H}) \quad (2)$$

It remains to determine at what times (if any) the  $\varphi_L = 0$  condition arises. To this end, consider the launch body-centered right-handed Cartesian NAH coordinate system defined by the following EPM unit vectors along with  $\mathbf{H}$ .

$$\text{Target orbit plane ascending node unit vector on launch body equator } \mathbf{N} = \text{unit}(\mathbf{K} \times \mathbf{H}) \quad (3)$$

$$\text{Target orbit plane northern anti-node versus launch body equator } \mathbf{A} = \mathbf{H} \times \mathbf{N} \quad (4)$$

Initially, ignore the time-dependent influence of  $\lambda_{AN}$  and focus on relating the launch site's declination on the launch body's equator<sup>3</sup> to the launch site's argument of latitude  $u_L$  in the target orbit plane. This is accomplished by first computing the target orbit's inclination on the launch body equator and the sine of launch site equatorial declination as follows.

$$i = \arccos(\mathbf{K} \cdot \mathbf{H}) \quad (5)$$

$$\sin \delta_L = \mathbf{K} \cdot \mathbf{R}_L \quad (6)$$

Assuming  $\lambda_{AN} = 0$  for the present, the westward-biased EPM-to-NAH transformation  $M_N^{\text{NAH}}$  results from two Euler rotations: a roll through  $+i$  followed by a yaw through  $+u_L$ .

$$M_N^{\text{NAH}} = \begin{bmatrix} \cos u_L & \sin u_L & 0 \\ -\sin u_L & \cos u_L & 0 \\ 0 & 0 & 1 \end{bmatrix} \begin{bmatrix} 1 & 0 & 0 \\ 0 & \cos i & \sin i \\ 0 & -\sin i & \cos i \end{bmatrix}$$

<sup>2</sup> All  $\text{atan2}$  results are assumed to reside in an interval equivalent to one from  $-180^\circ$  increasing through zero to  $+180^\circ$ . Also note that some  $\text{atan2}$  implementations, notably those in Excel spreadsheets, require argument ordering be reversed from that appearing herein.

<sup>3</sup> The term "declination" is used in this context because the "tail" of  $\mathbf{R}_L$  is at the launch body's center in Figure 1. Declination is generally distinct from "latitude" on an oblate body's surface such as Earth's. Oblate surface latitude is reckoned along a local vertical "plumb line" offset from the body's center except at the equator and along  $\mathbf{K}$ .

## Launch Site Geometric In-Plane Time On A Target Orbit

$$M_N^{\text{NAH}} = \begin{bmatrix} \cos u_L & \cos i \sin u_L & \sin i \sin u_L \\ -\sin u_L & \cos i \cos u_L & \sin i \cos u_L \\ 0 & -\sin i & \cos i \end{bmatrix} \quad (7)$$

Further assume in-plane launch site geometry exists such that  $R_{LH} = 0$  and apply Equation 7 as an inverse transformation to the launch site position unit vector in NAH coordinates.

$$\begin{bmatrix} R_{LN} \\ R_{LE} \\ R_{LK} \end{bmatrix} = [M_N^{\text{NAH}}]^T \begin{bmatrix} 1 \\ 0 \\ 0 \end{bmatrix} = \begin{bmatrix} \cos u_L \\ \cos i \sin u_L \\ \sin i \sin u_L \end{bmatrix} \quad (8)$$

In Equation 8, note  $R_{LN}$  is the component of  $\mathbf{R}_L$  along  $N$ , while  $R_{LE}$  is the equatorial component of  $\mathbf{R}_L$  directed  $90^\circ$  of longitude east of  $N$ . Equation 8 then leads to the time-independent launch site geometric in-plane criterion.

$$R_{LK} = \sin \delta_L = \sin i \sin u_L \Rightarrow u_L = \arcsin \left\{ \frac{\sin \delta_L}{\sin i} \right\} \quad (9)$$

If  $|\sin \delta_L|$  exceeds  $\sin i$ , Equation 9 cannot be evaluated because the launch site is *never* in the target orbit plane as the launch body rotates.<sup>4</sup> In such cases, set  $u_L = +90^\circ$  for positive  $\sin \delta_L$  or  $u_L = -90^\circ$  for negative  $\sin \delta_L$ . These Equation 9 proxy values place the launch site as close as possible to the nearest target orbit plane anti-node. Evaluate Equation 8 for  $R_{LN}$ ,  $R_{LE}$ , and  $R_{LK}$  accordingly.

For  $|\sin \delta_L| < \sin i$ , Equation 9 will generally provide two  $u_L$  solutions: one with the target orbit plane heading northbound over the launch site, and one with the heading southbound over the launch site. Most arc-sine function implementations will return  $u_L$  in Quadrant I for  $\sin \delta_L > 0$  and  $u_L$  in Quadrant IV for  $\sin \delta_L < 0$ . Both results correspond to a northbound target orbit plane heading. If a southbound heading is desired, subtract a Quadrant I Equation 9 result from  $+180^\circ$  or subtract a Quadrant IV Equation 9 result from  $-180^\circ$ . Evaluate Equation 8 for  $R_{LN}$ ,  $R_{LE}$ , and  $R_{LK}$  according to the northbound/southbound  $u_L$  selection.

For display purposes, it may be useful to compute the launch body-centered "phase angle"  $\theta$  between  $\mathbf{r}$  and  $\mathbf{R}_L$  projected into the target orbit plane at  $t_0$ . Thus,  $\theta$  is simply the difference between the selected  $u_L$  and the target position  $\mathbf{r}$ 's argument of latitude  $u_r$ .

$$\text{If } \mathbf{K} \cdot \mathbf{r} < 0, u_r = -\arccos \left\{ \frac{\mathbf{N} \cdot \mathbf{r}}{r} \right\}. \text{ Otherwise, } u_r = \arccos \left\{ \frac{\mathbf{N} \cdot \mathbf{r}}{r} \right\}. \quad (10)$$

By convention,  $\theta$  is required to assume values from zero to  $+360^\circ$ , but  $u_L$  and  $u_r$  can have values from  $-180^\circ$  through zero to  $+180^\circ$ , causing Equation 11 to produce  $\theta$  values from  $-360^\circ$  through

---

<sup>4</sup> This geometry arose for STS-61 and subsequent Hubble Space Telescope (HST) repair missions, even though they were launched from Kennedy Space Center (KSC) locations proximal to that of the STS-31 mission on which HST was originally deployed in orbit. At times, orbit perturbations are sufficient to place the HST orbit's northern anti-node slightly south of KSC locations when a repair mission is launched.

## Launch Site Geometric In-Plane Time On A Target Orbit

zero to  $+360^\circ$ . Consequently, a negative value from Equation 11 should be corrected by adding  $360^\circ$ .

$$\theta = u_r - u_L \quad (11)$$

Next, compute the co-longitude of  $\mathbf{R}_L$  with respect to  $N$ . Recall Footnote 2 applies to Equation 12.

$$\Delta\lambda_N = \text{atan2}(R_{LE}, R_{LN}) \quad (12)$$

Compute the target orbit plane's ascending node longitude  $\lambda_{AN}$  with Equation 13, again being mindful of Footnote 2.

$$\lambda_{AN} = \text{atan2}(N_J, N_I) \quad (13)$$

Use Equation 14 to compute the longitude shift required to place  $\mathbf{R}_L$  at the specified EPM longitude. Per Footnote 2, each term in Equation 14 may contribute as much as  $\pm 180^\circ$  to  $\Delta\lambda$ , thus producing values from  $-540^\circ$  to  $+540^\circ$ . But no longitude can be more than  $\pm 180^\circ$  from any other. Therefore, any Equation 14 result having  $\Delta\lambda < -180^\circ$  should be corrected by adding  $360^\circ$ . Likewise, any Equation 14 result having  $\Delta\lambda > +180^\circ$  should be corrected by subtracting  $360^\circ$ . These limiting operations tend to confine launch time estimates within a 24-hour interval.

$$\Delta\lambda = \lambda_L - \lambda_{AN} - \Delta\lambda_N \quad (14)$$

A corrected launch time is then determined. In Equation 15, note the second term's negative sign requires  $\Delta\lambda$  to decrease if  $t_L$  is to increase. Since the only time-dependent term in  $\Delta\lambda$  is  $\lambda_{AN}$ , an increase in  $t_L$  ultimately requires  $\lambda_{AN}$  to decrease as  $\omega$  shifts the target orbit ground track westward while the launch body rotates eastward.

$$t_L = t_0 - \Delta\lambda/\omega \quad (15)$$

If  $|\Delta\lambda|$  is less than a specified convergence threshold, further iteration is not necessary. Otherwise, another iteration evaluating Equations 1-15 is warranted starting with updates to  $\mathbf{r}$  and  $\mathbf{v}$  at a new  $t_0$  set to the corrected  $t_L$ . Even if  $\Delta\lambda$  is modest in magnitude, further iteration is advisable should the target ephemeris be subject to perturbations altering its orbit plane orientation in inertial space.

Note  $t_L$  may converge to a time unacceptably different from a time and date of interest. In such cases, initiate a new iteration with  $t_0$  changed to an appropriate integral number of launch body rotation periods before or after the unacceptable converged  $t_L$  value.

When implemented, the foregoing iterative  $t_L$  algorithm produces a starting point for further iterations using a launch vehicle-specific simulation. With this simulation, the effects of  $t_L$  on launch vehicle performance can be quantified and optimized as initial eastward inertial motion due to  $\omega$  at the launch site is propulsively turned to achieve the targeted orbit plane, altitude, and

## Launch Site Geometric In-Plane Time On A Target Orbit

flight path angle during powered ascent to a rendezvous phasing orbit. The simulation can further consider the effects of differential nodal regression due to gravitational perturbations on the phasing orbit and the target orbit at their respective altitudes. This consideration leads to targeting a "phantom plane" for the phasing orbit such that it becomes coplanar with the target orbit when  $\theta$  becomes zero.

To test the  $t_L$  algorithm, consider SpaceX Crew-10 *Dragon* launch from KSC LC-39A on 14 March 2025 at 23:03:48 UTC. This mission targeted docking with ISS on 16 March 2025.<sup>5</sup> An ISS ephemeris with initialization data supplied by Mission Control-Houston's Trajectory Operations and Planning Officer (TOPO) at 14.5 March 2025 UTC supplies target  $\mathbf{r}$  and  $\mathbf{v}$  vectors at a candidate  $t_0$ . Implemented in an Excel spreadsheet, each algorithm iteration for the test is captured in the following sequence of figures. Cells colored **cyan** are input values, and "Eq." annotations are references to Equations 1-15. The assumed  $t_0$  for each iteration appears in Cell B2, and the corrected  $t_L$  appears in Cell B40.

---

<sup>5</sup> Reference [https://en.wikipedia.org/wiki/SpaceX\\_Crew-10](https://en.wikipedia.org/wiki/SpaceX_Crew-10) (accessed 29 September 2025).

## Launch Site Geometric In-Plane Time On A Target Orbit

	A	B	C	D	E	F
1	rad/day $\omega$ =	6.30038736				
2	Launch UTC $t_0$ =	2025-03-14 @ 12:00:00				
3	Des="D"; Asc Otherwise =	A				
4			KSC LC-39A Launch Site Position EPM UV $RL$			Magnitude
5			0.143545773	-0.867465565	0.476338225	1
6	Launch Site EPM °Lon $\lambda_L$ =	-80.604				
7			km Target EPM Position $r$			
8			-3653.011	-5651.515	965.951	6798.321
9						
10			km/s Target EPM Velocity $v$			
11			3.565813	-3.326218	-5.905582	7.658632
12						
13			km <sup>2</sup> /s Target EPM Ang. Momentum $h = r \times v$			
14			36588.44951	-18128.75435	32302.95515	52065.7976
15						
16			Eq. 1: Target EPM Ang. Momentum UV $H$			
17			0.702734831	-0.348189314	0.620425627	1
18	Eq. 2: Launch Site NAH °Lat $\phi_L$ =	44.303				
19			Target Orbit EPM Node Vector $n = K \times H$			
20			0.348189314	0.702734831	0	0.78426529
21						
22			Eq. 3: Target Orbit EPM Node UV $N$			
23			0.443968794	0.896042248	0	1
24						
25			Eq. 4: Target Orbit EPM N Anti-Node UV $A = H \times N$			
26			-0.555927574	0.275449617	0.784265287	1
27	Eq. 5: $i$ =	51.653				
28	$\sin i$ =	0.784265287				
29	Eq. 6: $\sin \delta_L$ =	0.476338225				
30	Eq. 8: $RLN$ =	0.794420043				
31	Eq. 8: $RLE$ =	0.376827136				
32	Eq. 9: Preliminary °uL =	37.399				
33	Ascending °uL	37.399				
34	Eq. 10: °ur =	169.562				
35	Eq. 11: ° $\theta$ =	132.162				
36	Eq. 12: co-longitude ° $\Delta \lambda_N$ =	25.377				
37	Eq. 13: asc. node lon ° $\lambda_{AN}$ =	63.643				
38	Eq. 14: Prelim. lon correction ° $\Delta \lambda$ =	-169.624				
39	Limited ° $\Delta \lambda$ =	-169.624				
40	Eq. 15: corrected Launch UTC $t_L$ =	2025-03-14 @ 23:16:39				

**Figure 2. Iteration-1 is recorded from the Crew-10 launch test. Note the initial  $t_0$  in Cell B2 is deliberately set half a day before actual  $t_L$  to induce a large Iteration-1 correction by the algorithm.**

## Launch Site Geometric In-Plane Time On A Target Orbit

	A	B	C	D	E	F
1	rad/day $\omega$ =	6.30038736				
2	Launch UTC $t_0$ =	2025-03-14 @ 23:16:39				
3	Des="D"; Asc Otherwise =	A				
4			KSC LC-39A Launch Site Position EPM UV $RL$			Magnitude
5			0.143545773	-0.867465565	0.476338225	1
6	Launch Site EPM °Lon $\lambda_L$ =	-80.604				
7			km Target EPM Position $r$			
8			-4119.455	973.774	-5323.008	6800.924
9						
10			km/s Target EPM Velocity $v$			
11			-2.151386	-7.332943	0.329427	7.649120
12						
13			km <sup>2</sup> /s Target EPM Ang. Momentum $h = r \times v$			
14			-38712.52652	12808.90465	32302.69637	52021.0721
15						
16			Eq. 1: Target EPM Ang. Momentum UV $H$			
17			-0.744170102	0.246225311	0.620954069	1
18	Eq. 2: Launch Site NAH °Lat $\phi_L$ =	-1.411				
19			Target Orbit EPM Node Vector $n = K \times H$			
20			-0.246225311	-0.744170102	0	0.78384695
21						
22			Eq. 3: Target Orbit EPM Node UV $N$			
23			-0.314124218	-0.949381891	0	1
24						
25			Eq. 4: Target Orbit EPM N Anti-Node UV $A = H \times N$			
26			0.589522548	-0.195056711	0.783846952	1
27	Eq. 5: $^\circ i$ =	51.614				
28	$\sin i$ =	0.783846952				
29	Eq. 6: $\sin \delta_L$ =	0.476338225				
30	Eq. 8: $RLN$ =	0.794172112				
31	Eq. 8: $RLE$ =	0.377349377				
32	Eq. 9: Preliminary $^\circ u_L$ =	37.423				
33	Ascending $^\circ u_L$	37.423				
34	Eq. 10: $^\circ u_r$ =	-86.885				
35	Eq. 11: $^\circ \theta$ =	235.692				
36	Eq. 12: co-longitude $^\circ \Delta \lambda_N$ =	25.415				
37	Eq. 13: asc. node lon $^\circ \lambda_{AN}$ =	-108.308				
38	Eq. 14: Prelim. lon correction $^\circ \Delta \lambda$ =	2.289				
39	Limited $^\circ \Delta \lambda$ =	2.289				
40	Eq. 15: corrected Launch UTC $t_L$ =	2025-03-14 @ 23:07:31				

**Figure 3. Iteration-2 is recorded from the Crew-10 launch test. Note  $t_0$  in Cell B2 is set to the corrected  $t_L$  from Iteration-1. In Cell B39, note  $\Delta \lambda$ 's convergence towards zero with respect to Figure 2.**



## Launch Site Geometric In-Plane Time On A Target Orbit

	A	B	C	D	E	F
1	rad/day $\omega$ =	6.30038736				
2	Launch UTC $t_0$ =	2025-03-14 @ 23:07:31				
3	Des="D"; Asc Otherwise =	A				
4			KSC LC-39A Launch Site Position EPM UV $RL$			Magnitude
5			0.143545773	-0.867465565	0.476338225	1
6	Launch Site EPM °Lon $\lambda_L$ =	-80.604				
7			km Target EPM Position $r$			
8			-2437.218	4470.195	-4511.463	6802.644
9						
10			km/s Target EPM Velocity $v$			
11			-4.213505	-5.525699	-3.197003	7.649039
12						
13			km <sup>2</sup> /s Target EPM Ang. Momentum $h = r \times v$			
14			-39220.2081	11217.27764	32302.52298	52033.6913
15						
16			Eq. 1: Target EPM Ang. Momentum UV $H$			
17			-0.753746411	0.215577203	0.620800142	1
18	Eq. 2: Launch Site NAH °Lat $\phi_L$ =	0.029				
19			Target Orbit EPM Node Vector $n = K \times H$			
20			-0.215577203	-0.753746411	0	0.78396887
21						
22			Eq. 3: Target Orbit EPM Node UV $N$			
23			-0.274981842	-0.96144942	0	1
24						
25			Eq. 4: Target Orbit EPM N Anti-Node UV $A = H \times N$			
26			0.596867937	-0.170708767	0.783968866	1
27	Eq. 5: $\circ i$ =	51.625				
28	$\sin i$ =	0.783968866				
29	Eq. 6: $\sin \delta_L$ =	0.476338225				
30	Eq. 8: $RLN$ =	0.794244415				
31	Eq. 8: $RLE$ =	0.37719717				
32	Eq. 9: Preliminary °uL =	37.416				
33	Ascending °uL	37.416				
34	Eq. 10: °ur =	-122.227				
35	Eq. 11: ° $\theta$ =	200.357				
36	Eq. 12: co-longitude ° $\Delta \lambda N$ =	25.404				
37	Eq. 13: asc. node lon ° $\lambda_{AN}$ =	-105.961				
38	Eq. 14: Prelim. lon correction ° $\Delta \lambda$ =	-0.047				
39	Limited ° $\Delta \lambda$ =	-0.047				
40	Eq. 15: corrected Launch UTC $t_L$ =	2025-03-14 @ 23:07:42				

**Figure 4. Iteration-3 is recorded from the Crew-10 launch test. Note  $t_0$  in Cell B2 is set to the corrected  $t_L$  from Iteration-2. With  $\Delta \lambda = -0.047^\circ$  in Cell B39, Iteration-3's corrected  $t_L$  in Cell B40 is deemed converged.**

Typical Space Shuttle missions targeting ISS rendezvous had certified planar steering capability spanning launch windows 10 minutes in duration. The Figure 4  $t_L$  result, only 3.9 minutes later than actual, would therefore seed a plausible, if non-optimal, Crew-10 launch vehicle simulation under nominal conditions in lieu of a specified launch date and time.

Recalling Footnote 4, a fictitious launch from KSC LC-39B on 16 September 2025 targeting HST rendezvous is used to further test the  $t_L$  algorithm. This is indeed a stress test because HST



## Launch Site Geometric In-Plane Time On A Target Orbit

was originally launched due east from LC-39A about  $0.019^\circ$  south of the test's  $R_L$ . Consequently, logic dealing with  $|\sin \delta_L| > \sin i$  in Equation 9 is apt to be triggered. No less than five iterations are required in converging to a northbound HST in-plane time at 21:01:32 UTC from a  $t_0 = 12:00:00$  UTC specified for Iteration-1. Primary among causes of the HST test's protracted iterations is  $u_L$  inconsistency as summarized in Table 1.

**Table 1. Inconsistencies in  $u_L$  triggered by  $\sin \delta_L$  very nearly equal to  $\sin i$  in Equation 9 are summarized for the HST test's five iterations. A proxy  $u_L$  value of exactly  $+90^\circ$  indicates Equation 9 cannot be evaluated because no in-plane geometry exists. The  $t_0$  column pertains to estimated launch on 16 September 2025.**

Iteration	$t_0$ (UTC)	$^\circ u_L$
1	12:00:00	+90
2	21:20:26	+90
3	21:09:55	+88.002
4	21:00:59	+88.205
5	21:01:55	+88.125

Although  $\sin \delta_L$  is a constant  $+0.476628711$  throughout the HST test,  $\sin i$  has minute variations from one iteration to another. These variations arise because the HST ephemeris being used reflects perturbations to conic geocentric motion. Chief among perturbations acting on the HST orbit plane is Earth's " $J_2$ " excess equatorial mass. As illustrated in Figure 5, fetching  $r$  and  $v$  from the ephemeris when HST is at near-equatorial EPM declinations (**orange** sinusoidal curve and scale at right) causes Equation 5 to produce EPM inclinations (**blue** sinusoidal curve and scale at left) with higher values than when ephemeris sampling occurs with HST farther from Earth's equator.

Also referred to Figure 5's **blue** scale is the solid **blue** horizontal line at  $28.465448^\circ$ . This is the time-independent EPM declination of LC-39B,  $\delta_L$ . When a candidate in-plane time  $t_0$  corresponds to an HST inclination greater than  $\delta_L$ , a northbound or southbound in-plane time exists. Otherwise,  $u_L$  must be fixed at  $+90^\circ$  for LC-39B to obtain a planar closest approach launch time. For reference, the converged in-plane time from Iteration-5 coincides with the vertical dotted **black** line in Figure 5. Note the Iteration-2  $t_0$  from Table 1 produces a sub- $\delta_L$  EPM inclination of  $28.464835^\circ$  in Figure 5, thus triggering a  $u_L = +90^\circ$  proxy.

## Launch Site Geometric In-Plane Time On A Target Orbit

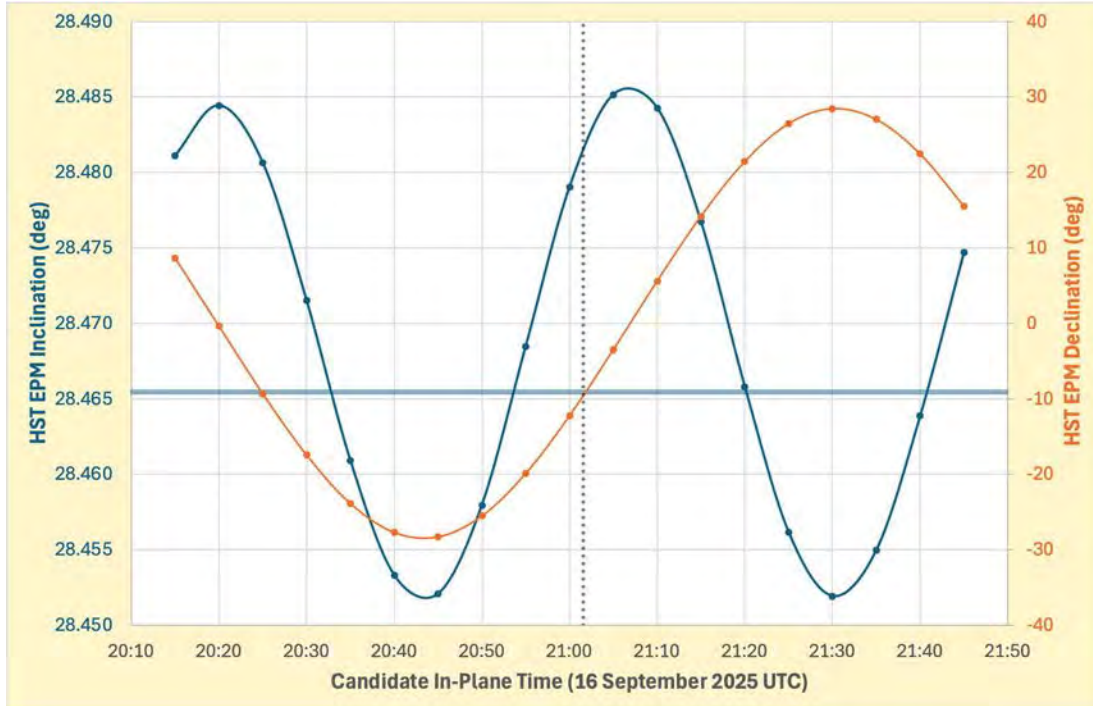


**Figure 5.** The relationship between perturbed HST inclination (blue curve and scale at left) and HST declination (orange curve and scale at right) is apparent during the orbit period interval centered near converged northbound in-plane time (vertical dotted black line) for KSC LC-39B. At a UTC when HST inclination falls below the horizontal blue line at LC-39B's EPM declination, no in-plane time exists, and a proxy  $u_L$  value of  $+90^\circ$  is required.

Tangential geometry between the HST ground track and KSC's location on the Florida east coast at the converged in-plane time of launch on 16 September 2025 is evident in Figure 6. This illustration serves as a sanity check on the HST test's result, including the Iteration-5  $\theta$  value of  $252.821^\circ$ .

## Launch Site Geometric In-Plane Time On A Target Orbit

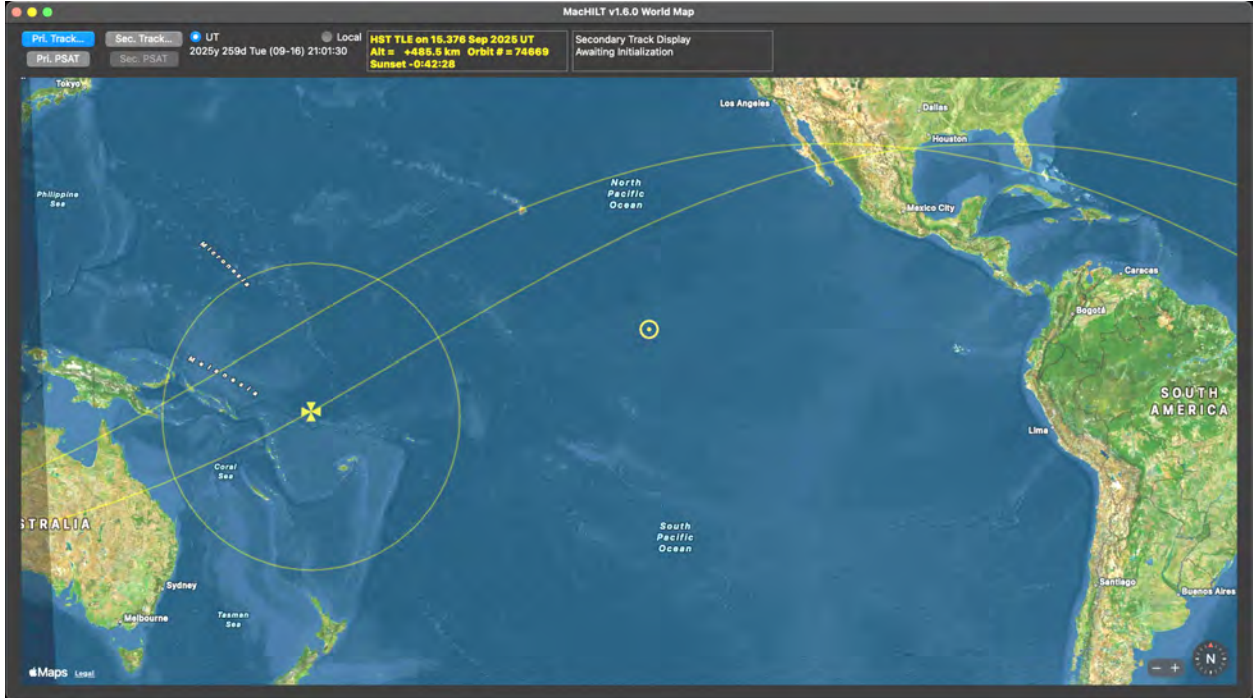


**Figure 6.** At the converged KSC LC-39B in-plane launch time of 21:01:32 UTC on 16 September 2025, HST's location over the southwest Pacific Ocean is denoted by the yellow Maltese cross marker ✕. This launch geometry places HST nearly  $253^\circ$  in easterly orbit plane motion "ahead" of the launch site on Florida's east coast. Note how eastward Earth rotation moves the launch site nearly tangential to HST's yellow ground track as that trajectory crosses the Florida peninsula. A yellow ☉ icon in the mid-Pacific Ocean denotes the sub-solar point on Earth's surface at launch.

## Epilogue: Planar Steering Considerations

The plane to be achieved following post-launch powered flight steering can be approximated by the rendezvous target orbit plane's normal  $\mathbf{H}$ .<sup>6</sup> But what about the many mission scenarios in which there are no rendezvous constraints? In those cases,  $t_L$  is fixed by other considerations such as lighting and weather-driven launch probability. Although  $i$  is typically specified even when there is no rendezvous plane,  $\mathbf{H}$  cannot be computed with Equation 1 because there is no target vehicle ephemeris from which to obtain  $\mathbf{r}$  and  $\mathbf{v}$ . How then is  $\mathbf{H}$  obtained to support planar steering?

Of course,  $\mathbf{R}_L$  is known, and range safety considerations will typically dictate a northbound or southbound launch azimuth. This permits Equations 6 through 9 to be evaluated, producing a value for  $u_L$  limited to the interval  $\pm 180^\circ$ . Equation 12 then determines the launch site's co-longitude  $\Delta\lambda_N$  with respect to the desired orbit plane's ascending node on the EPM equator. As before,  $\Delta\lambda_N$  should be limited to the interval  $\pm 180^\circ$ .

<sup>6</sup> Space Shuttle flight software used  $-\mathbf{H}$  at Main Engine Cutoff (MECO), expressed with Cartesian components in the geocentric Earth Mean Equator and Equinox of Besselian epoch B1950.0 coordinate system, as planar steering parameters during Ascent Guidance.

## Launch Site Geometric In-Plane Time On A Target Orbit

To preserve the launch site's known longitude  $\lambda_L$ , Equation 16 must be evaluated so  $\lambda_{AN}$  is consistent per Figure 1's geometry. For display purposes,  $\lambda_{AN}$  from Equation 16 can be limited to the interval  $\pm 180^\circ$  by adding or subtracting  $360^\circ$  to the initial result as necessary, but enforcement of this convention will not affect  $\mathbf{H}$  in Equation 18.

$$\lambda_L = \lambda_{AN} + \Delta\lambda_N \Rightarrow \lambda_{AN} = \lambda_L - \Delta\lambda_N \quad (16)$$

The EPM-to-node transformation  $M_{EPM}^N$  is then computed as a yaw through  $+\lambda_{AN}$  followed by a roll through  $+i$ .

$$M_{EPM}^N = \begin{bmatrix} 1 & 0 & 0 \\ 0 & \cos i & \sin i \\ 0 & -\sin i & \cos i \end{bmatrix} \begin{bmatrix} \cos \lambda_{AN} & \sin \lambda_{AN} & 0 \\ -\sin \lambda_{AN} & \cos \lambda_{AN} & 0 \\ 0 & 0 & 1 \end{bmatrix}$$

$$M_{EPM}^N = \begin{bmatrix} \cos \lambda_{AN} & \sin \lambda_{AN} & 0 \\ \cos \lambda_{AN} \cos i & \cos \lambda_{AN} \sin i & \sin i \\ \sin \lambda_{AN} \cos i & \sin \lambda_{AN} \sin i & \cos i \end{bmatrix} \quad (17)$$

When the inverse  $M_{EPM}^N$  transformation is applied to the desired plane's normal unit vector in  $N$  coordinates, the vector required for planar steering in EPM coordinates results.

$$\mathbf{H} \equiv \begin{bmatrix} H_I \\ H_J \\ H_K \end{bmatrix} = [M_{EPM}^N]^T \begin{bmatrix} 0 \\ 0 \\ 1 \end{bmatrix} = \begin{bmatrix} \sin \lambda_{AN} \sin i \\ -\cos \lambda_{AN} \sin i \\ \cos i \end{bmatrix} \quad (18)$$

To test Equations 16 and 18, values from Figure 4 are used.

$\lambda_L = -80.604^\circ$  (reference Cell B6)

$i = 51.625^\circ$  (reference Cell B27)

$\Delta\lambda_N = +25.404^\circ$  (reference Cell B36)

$\lambda_{AN} = -106.008^\circ$  (reference Equation 16 and compare to Cell B37 =  $-105.961^\circ$ )

$H_I = -0.753565$  (reference Equation 18 and compare to Cell C17 =  $-0.753746$ )

$H_J = +0.216195$  (reference Equation 18 and compare to Cell D17 =  $+0.215577$ )

$H_K = +0.620806$  (reference Equation 18 and compare to Cell E17 =  $+0.620800$ )

In practice, it may be desirable to add a signed user-specified  $\lambda_{AN}$  bias term  $\varepsilon$  to Equation 16. With several launch simulations, each having its own trial  $\varepsilon$  value, the  $\mathbf{H}$  leading to minimum launch vehicle propellant consumption can be determined to the desired precision. In the context of easterly prograde launches from Earth, optimal  $\varepsilon$  is typically positive (eastward) and one or two degrees in magnitude depending on  $i$  and  $\delta_L$ . This bias provides leeway for sufficient powered ascent steering northward or southward of the launch site before the desired plane is encountered, thus avoiding a wasteful double-dogleg "east to west to east" ground track.